Inorg. Chem. **2002**, *41*, 4756–4762

Characterization of a Soluble Molecular Magnet: Unusual Magnetic Behavior of Cyano-Bridged Gd(III)–Cr(III) Complexes with One-Dimensional and Nanoscaled Square Structures

Hui-Zhong Kou,*,† Song Gao,‡ Chun-Hui Li,† Dai-Zheng Liao,§ Bei-Chuan Zhou,† Ru-Ji Wang,† and Yadong Li†

Department of Chemistry, Tsinghua University, Beijing 100084, P.R. China, State Key Laboratory of Rare Earth Materials Chemistry and Applications, Peking University, Beijing 100871, P.R. China, and Department of Chemistry, Nankai University, Tianjin 300071, P.R. China

Received May 8, 2002

Two cyano-bridged Gd(III)–Cr(III) complexes $[Gd(urea)_4(H_2O)_2]_2[Cr(CN)_6]_2$ (**1**) and $\{[Gd(capro)_2(H_2O)_4Cr(CN)_6]\cdot H_2O\}_n$ (**2**) (capro represents caprolactam) have been synthesized and characterized structurally and magnetically. Complex **1** has a tetranuclear Gd_2Cr_2 square structure, in which two *cis*-CN^- ligands of each $[Cr(CN)_6]$ link two $[Gd(urea)_4(H_2O)_2]$ groups and in turn, two $[Gd(urea)_4(H_2O)_2]$ link two $[Cr(CN)_6]$ in a *cis* fashion. Complex **2** is composed of 1D chains with alternating $[Gd(capro)_2(H_2O)_4]$ and $[Cr(CN)_6]$ moieties connected by the *trans*-CN^- ligands of $[Cr(CN)_6]$. The dehydration of **2** at 120 °C generates a new complex, $[Gd(capro)_2(H_2O)_2Cr(CN)_6]$ (**2′**). Magnetic studies show the existence of antiferromagnetic Gd(III)–Cr(III) interaction in these complexes. On the basis of the tetranuclear model, the magnetic susceptibilities of **1** have been analyzed giving the intermetallic magnetic coupling constant of –0.36 cm^{-1}. Complex **2′** exhibits a ferrimagnetic order below 2.1 K. Interestingly, **2′** is quite soluble in water, and slow evaporation of the solution gives the hydrated complex **2**. Therefore, **2′** is a soluble molecular magnet, and this significant behavior implies potential applications. Isothermal magnetization measurements of **2′** and other cyano-bridged Gd(III)–Cr(III) molecular magnets show unusual field-induced metamagnetic behavior from the ferrimagnetic ground state to the ferromagnetic state. Field dependence of magnetization of the cyano-bridged Gd(III)–Cr(III) complexes shows unusual field-induced metamagnetic behavior from the ferrimagnetic ground state to the ferromagnetic state.

Introduction

The magnetochemistry of transition metal complexes was greatly advanced. This can be represented by the characterization of room-temperature molecular magnets,[1] single molecule magnets,[2] magnetooptical materials,[3] and those with spin-crossover phenomena,[4] which might find their applications useful for information storage or displays. The attracting features of these molecular magnets lie in (1) various molecular structures to be designed,[5−7] (2) the optical transparency of the molecular magnets, and (3) magnetic solubility in water or organic solvents. Among these,

* To whom correspondence should be addressed. E-mail: kouhz@mail.tsinghua.edu.cn. Fax: 86-10-62788765.

† Tsinghua University.

‡ Peking University.

§ Nankai University.

(1) Holmes, S. M.; Girolami, G. S. *J. Am. Chem. Soc*. **1999**, *121*, 5593. Ferlay, S.; Mallah, T.; Ouahes, R.; Veillet, P.; Verdaguer, M. *Nature* **1995**, *378*, 701. Dujardin, E.; Ferlay, S.; Phan, X.; Desplanches, C.; Cartier dit Moulin C.; Sainctavit, P.; Baudelet, F.; Dartyge, E.; Verdaguer, M. *J. Am. Chem. Soc*. **1998**, *120*, 11347. Pokhodnya, K. I.; Pejakovic, D.; Epstein, A. J.; Miller, J. S. *Phys. Rev. B* **2001**, *63*, 174408. Hatlevik, *φ*.; Buschmann, W. E.; Zhang, J.; Manson, J. L.; Miller, J. S. *Adv. Mater*. **1999**, *11*, 914.

(2) Boskovic, C.; Pink, M.; Huffman, J. C.; Hendrickson, D. N.; Christou, G. *J. Am. Chem. Soc*. **2001**, *123*, 9914. Castro, S. L.; Sun, Z.; Grant, C. M.; Bollinger, J. C.; Hendrickson, D. N.; Christou, G. *J. Am. Chem. Soc*. **1998**, *120*, 2365. Aubin, S. M. J.; Dilley, N. R.; Wemple, M.; Maple, M. B.; Christou, G.; Hendrickson, D. N. *J. Am. Chem. Soc*. **1998**, *120*, 839. Zhong, Z. J.; Seino, H.; Mizobe, Y.; Hidai, M.; Fujishima, A.; Ohkoshi, S.; Hashimoto, K. *J. Am. Chem. Soc*. **2000**, *122*, 2952.

(3) Sato, O.; Iyoda, T.; Fujishima, A.; Hashimoto, K. *Science* **1996**, *271*, 49. Sato, O.; Einaga, Y.; Fujishima, A.; Hashimoto, K. *Inorg. Chem*. **1999**, *38*, 4405. Gu, Z. Z.; Einaga, Y.; Sato, O.; Fujishima, A.; Hashimoto, K. *J. Solid State Chem*. **2001**, *159*, 336. Bleuzen, A.; Lomenech, C.; Escax, V.; Villain, F.; Varret, F.; Moulin, C. C. D.; Verdaguer, M. *J. Am. Chem. Soc*. **2000**, *122*, 6648.

(4) Breuning, E.; Ruben, M.; Lehn, J. M.; Renz, F.; Garcia, Y.; Ksenofontov, V.; Gutlich, P.; Wegelius, E.; Rissanen, K. *Angew. Chem., Int. Ed*. **2000**, *39*, 2504. Hayami, S.; Gu, Z. Z.; Yoshiki, H.; Fujishima, A.; Sato, O. *J. Am. Chem. Soc*. **2001**, *123*, 11644.

10.1021/ic025704j CCC: $22.00
Published on Web 08/01/2002

solubility of magnets has obvious benefits in future technological applications that might require, for example, thin films. However, most of the reported molecular magnets are not soluble, especially the polymeric magnets. The search for soluble magnets remains a challenge.

Lanthanide(III) hexacyanoferrates and the analogous chromium(III) complexes form a family of magnetic materials.[8−11] Recently, we have designed and prepared two cyano-bridged 2D brick-wall-like bimetallic complexes $[Ln(DMF)_2(H_2O)_3Cr(CN)_6]\cdot H_2O$ (Ln = Sm, Gd) with long-range magnetic ordering at low temperatures, which serve as the only examples of 2D 4f−3d species exhibiting spontaneous magnetization.[10a,c] Interestingly, 1D 4f−3d complexes $[Ln(DMF)_4(H_2O)_2Mn(CN)_6]\cdot H_2O$ (Ln = Sm, Er) exhibit long-range magnetic ordering,[11] whereas the isostructural LnCr (Ln = Nd, Gd, Sm, Eu, Tb) complexes do not show magnetic ordering down to 2 K.[10b,c,12] Besides this, cyano-bridged 4f−3d compounds have been rarely magnetically investigated because of the complexity of magnetism of Ln^{3+} except that of the isotropic Gd^{3+} ion.[13−15] It is worth mentioning that the above-mentioned 2D 4f−3d magnets are soluble in water; however, slow evaporation of the resulting solution could not lead to the original complexes because of the ready loss of the solvent ligand (DMF). We infer that the replacement of DMF by larger molecule ligands might produce soluble and retrievable molecular magnets. In this paper, we report our findings along this line.

As far as cyano-bridged Gd(III)−Cr(III) complexes are concerned, it has been shown that the Gd(III)−Cr(III) exchange magnetic interaction is unambiguously antiferromagnetic.[8,10a,b] The magnitude of the magnetic coupling could not, however, be accurately evaluated because of the absence of a suitable model for the extended polymers. Therefore, a cyclic tetranuclear system, for example, a molecular square, can be used for this purpose as the simple model for infinite assemblies. Similar situations have appeared in the evaluation of the magnetic exchange in the 3D Prussian blue analogues, which have been analyzed through magnetic studies on polynuclear models.[16] To this end, we have isolated a tetranuclear square using urea as the ligand. In this paper, we report the synthesis, structures, and magnetic properties of the tetranuclear square $[Gd(urea)_4(H_2O)_2]_2[Cr(CN)_6]_2$ and 1D chain $\{[Gd(capro)_2(H_2O)_4Cr(CN)_6]\cdot H_2O\}_n$ (capro represents caprolactam).

Experimental Section

Elemental analyses of carbon, hydrogen, and nitrogen were carried out with an Elementar Vario EL. The infrared spectroscopy on KBr pellets was performed on a Magna-IR 750 spectrophotometer in the 4000−400 cm^{-1} region. TGA measurement of **2** was performed in the temperature range 20−300 °C under nitrogen on a Universal V2.6D TA instrument. Variable-temperature magnetic susceptibility measurements of **1** were performed on a Quantum Design MPMS SQUID magnetometer. Field-cooled magnetization (FCM), zero-field-cooled magnetization (ZFCM), and field dependence magnetization measurements of **1** and **2′** and variable-temperature magnetic susceptibility, zero-field AC magnetic susceptibility, and field dependence magnetization measurements of **2** were performed on a Maglab System^{2000} magnetometer. Effective

(5) 0D magnets: Larionova, J.; Gross, M.; Pilkington, M.; Audres, H.; Stoeckli-Evans, H.; Gudel, H. U.; Decurtins, S. *Angew. Chem., Int. Ed*. **2000**, *39*, 1605. Langenberg, K. V.; Batten, S. R.; Berry, K. J.; Hockless, D. C. R.; Moubaraki, B.; Murray, K. S. *Inorg. Chem*. **1997**, *36*, 5006. Vostrikova, K. E.; Luneau, D.; Wernsdorfer, W.; Rey, P.; Verdaguer, M. *J. Am. Chem. Soc*. **2000**, *122*, 718.

(6) Selected references for 1D magnets: Ohba, M.; Maruone, N.; Okawa, H.; Enoki, T.; Latour, J.-M. *J. Am. Chem. Soc*. **1994**, *116*, 11566. Marvillers, A.; Parsons, S.; Riviere, E.; Audiere, J.-P.; Mallah, T. *Chem. Commun*. **1999**, 2217. Matsumoto, N.; Sunatsuki, Y.; Miyasaka, H.; Hashimoto, Y.; Luneau, D.; Tuchagues, J.-P. *Angew. Chem., Int. Ed.* **1999**, *38*, 171. Hibbs, W.; Rittenberg, D. K.; Sugiura, K.; Burkhart, B. M.; Morin, B. G.; Arif, A. M.; Liable-Sands, L.; Rheingold, A. L.; Sundaralingam, M.; Epstein, A. J.; Miller, J. S. *Inorg. Chem.* **2001**, *40*, 1915. Sugiura, K.; Mikami, S.; Johnson, M. T.; Raebiger, J. W.; Miller, J. S.; Iwasaki, K.; Okada, Y.; Hino, S.; Sakata, Y. *J. Mater. Chem.* **2001**, *11*, 2152. Colacio, E.; Ghazi, M.; Stoeckli-Evans, H.; Lloret, F.; Moreno, J. M.; Perez, C. *Inorg. Chem.* **2001**, *40*, 4876. Selected references for 2D magnets: Manson J. L.; Huang, Q. Z.; Lynn, J. W.; Koo, H. J.; Whangbo, M. H.; Bateman, R.; Otsuka, T.; Wada, N.; Argyriou, D. N.; Miller, J. S. *J. Am. Chem. Soc.* **2001**, *123*, 162. Ohba, M.; Okawa, H.; Fukita, N.; Hashimoto, Y. *J. Am. Chem. Soc*. **1997**, *119*, 1011. Kou, H.-Z.; Gao, S.; Ma, B.-Q.; Liao, D.-Z. *Chem. Commun*. **2000**, 1309. Kou, H.-Z.; Gao, S.; Ma, B.-Q.; Liao, D.-Z. *Chem. Commun*. **2000**, 713. Kou, H.-Z.; Tang, J.-K.; Liao, D.-Z.; Gao, S.; Cheng, P.; Jiang, Z.-H.; Yan, S.-P.; Wang, G.-L.; Chansou, B.; Tuchagues, J.-P. *Inorg. Chem.* **2001**, *40*, 4839. Larionova, J.; Kahn, O.; Golhen, S.; Ouahab, L.; Clerac, R. *J. Am. Chem. Soc*. **1999**, *121*, 3349. Miyasaka, H.; Matsumoto, N.; Okawa, H.; Re, N.; Gallo, E.; Floriani, C. *J. Am. Chem. Soc*. **1996**, *118*, 981. Smith, J. A.; Galan-Mascaros, J.-R.; Clerac, R.; Dunbar, K. R. *Chem. Commun.* **2000**, 1077.

(7) Selected references for 3D magnets: Fallah, M. S. El; Rentschler, E.; Caneschi, A.; Sessoli, R.; Gatteschi, D. *Angew. Chem., Int. Ed. Engl*. **1996**, *35*, 1947. Ohba, M.; Usuki, N.; Fukita, N.; Okawa, H. *Angew. Chem., Int. Ed.* **1999**, *38*, 1795. Zhang, S.-W.; Fu, D.-G.; Sun, W.-Y.; Hu, Z.; Yu, K.-B.; Tang, W.-X. *Inorg. Chem*. **2000**, *39*, 1142. Kou, H.-Z.; Gao, S.; Zhang, J.; Wen, G.-H.; Su, G.; Zheng, R. K.; Zhang, X. X. *J. Am. Chem. Soc.* **2001**, *123*, 11809. Zhong, Z. J.; Seino, H.; Mizobe, Y.; Hidai, M.; Verdaguer, M.; Ohkoshi, S.; Hashimoto, K. *Inorg. Chem*. **2000**, *39*, 5095. Larionova, J.; Kahn, O.; Golhen, S.; Ouahab, L.; Clerac, R. *J. Am. Chem. Soc*. **1998**, *120*, 13088. Han, S.; Manson, J. L.; Kim, J.; Miller, J. S. *Inorg. Chem*. **2000**, *39*, 4182. Inoue, K.; Imai, H.; Ghalsasi, P. S.; Kikuchi, K.; Ohba, M.; Okawa, H.; Yakhmi, J. V. *Angew. Chem., Int. Ed.* **2001**, *40*, 4242.

(8) Hulliger, F.; Landolt, M.; Vetsch, H. *J. Solid State Chem.* **1976**, *18*, 283.

(9) Gao, S.; Ma, B.-Q.; Wang, Z.-M.; Yi, T.; Liao, C.-S.; Yan, C.-H.; Xu, G.-X. *Mol. Cryst. Liq. Cryst.* **1999**, *335*, 201. Ma, B.-Q.; Gao, S.; Su, G.; Xu, G.-X. *Angew. Chem., Int. Ed.* **2001**, *40*, 434. Gao, S.; Su, G.; Yi, T.; Ma, B.-Q. *Phys. Rev. B* **2001**, *63*, 054432.

(10) (a) Kou, H.-Z.; Gao, S.; Sun, B.-W.; Zhang, J. *Chem. Mater*. **2001**, 13, 1431. (b) Figuerola, A.; Diaz, C.; El Fallah, M. S.; Ribas, J.; Maestro, M.; Mahia, J. E. *Chem. Commun.* **2001**, 1204. (c) Kou, H.-Z.; Gao, S.; Jin, X. *Inorg. Chem*. **2001**, *40*, 6295.

(11) Yan, B.; Chen, Z. D.; Wang, S. X. *Transition Met. Chem. (Dordrecht, Neth.)* **2001**, *26*, 287. Yan, B.; Chen, Z. D.; Wang, S. X.; Gao, S. *Chem. Lett*. **2001**, 350.

(12) Kou, H.-Z.; Gao, S. Unpublished results.

(13) Garcia-Granda, S.; Morales, A. D.; Ruiz, E. R.; Bertran, J. F. *Acta Crystallogr*. **1996**, *C52*, 1679. Yi, T.; Gao, S.; Chen, X. W.; Yan, C. H.; Li, B. G. *Acta Crystallogr*. **1998**, *C54*, 41. Yang, C.; Gu, G. C.; Ma, H. W.; Liu, J. C.; Zhang, X.; Zheng, F. K.; Lin, S. H.; Zhou, G. W.; Mao, J. G.; Huang, J. S. *Jiegou Huaxue* **2001**, *20*, 229.

(14) Kou, H.-Z.; Yang, G.-M.; Liao, D.-Z.; Cheng, P.; Jiang, Z.-H.; Yan, S.-P.; Huang. X.-Y.; Wang, G.-L. *J. Chem. Crystallogr*. **1998**, *28*, 303. Kautz, J. A.; Mullica, D. F.; Cunningham, B. P.; Combs, R. A.; Farmer, J. M. *J. Mol. Struct*. **2000**, *523*, 175. Cunningham, B. P.; Kautz, J. A. *J. Chem. Crystallogr*. **2000**, *30*, 671. Combs, R. A.; Farmer, J. M.; Kautz, J. A. *Acta Crystallogr*. **2000**, *C56*, 1420.

(15) Liu, J. P.; Knoeppel, D. W.; Liu, S. M.; Meyers, E. A.; Shore, S. G. *Inorg. Chem*. **2001**, *40*, 2842. Knoeppel, D. W.; Shore, S. G. *Inorg. Chem*. **1996**, *35*, 5328. Knoeppel, D. W.; Liu, J.; Meyers, E. A.; Shore, S. G. *Inorg. Chem*. **1998**, *37*, 4828. Du, B.; Meyers, E. A.; Shore, S. G. *Inorg. Chem*. **2000**, *39*, 4639.

(16) Rogez, G.; Marvilliers, A.; Riviere, E.; Audiere, J. P.; Lloret, F.; Varret, F.; Goujon, A.; Mendenez, N.; Girerd, J. J.; Mallah, T. *Angew. Chem., Int. Ed*. **2000**, *39*, 2885. Parker, R. J.; Spiccia, L.; Berry, K. J.; Fallon, G. D.; Moubaraki, B.; Murray, K. S. *Chem. Commun.* **2001**, 333.

Table 1. Crystallographic Data for Complexes **1** and **2**

	1	**2**
formula	$C_{20}H_{40}Cr_2N_{28}O_{12}Gd_2$	$C_{18}H_{32}CrGdN_8O_7$
fw	1283.30	681.77
ë/Å	0.71073	0.71073
space group	$P\bar{1}$	$P2_1/n$
a/Å	8.6163(17)	11.0400(2)
b/Å	11.521(6)	14.7666(3)
c/Å	12.692(3)	17.1953(2)
α/deg	95.97(3)	90.00
β/deg	107.34(2)	92.3252(10)
γ/deg	98.25(3)	90.00
V/Å^3	1175.7(7)	2800.93(8)
Z	1	4
ρ_{calcd}/g cm^{-3}	1.813	1.617
μ(Mo Kα)/mm^{-1}	3.313	2.784
independent reflns	4115	8042
data/restraints/params	4115/0/299	8042/0/356
R1 [$I > 2\sigma(I)$]	0.0458	0.0322
wR2 (all data)	0.1405	0.0632

magnetic moments were calculated by the equation $\mu_{eff} = 2.828(\chi_m T)^{1/2}$, where χ_m is the molar magnetic susceptibility. The experimental susceptibilities were corrected for the diamagnetism of the constituent atoms (Pascal's Tables).

Syntheses. All chemicals and solvents used in the synthesis were reagent grade. The precursor $K_3[Cr(CN)_6]$ was prepared by the literature method.[17]

$[Gd(urea)_4(H_2O)_2]_2[Cr(CN)_6]_2$ (1). Yellow single crystals were obtained by slow evaporation of an aqueous solution (10 mL) of $GdCl_3 \cdot 6H_2O$, urea, and $K_3[Cr(CN)_6]$ in a molar ratio of 1:4:1. Anal. Calcd for $C_{20}H_{40}Cr_2Gd_2N_{28}O_{12}$: C, 18.72; H, 3.14; N, 30.56. Found: C, 19.02; H, 3.40; N, 30.18. IR (cm^{-1}): 2159, 2151, 2131 ($\nu_{C/N}$); 1649s, 1639sh ($\nu_{C=O}$).

$[Gd(capro)_2(H_2O)_4Cr(CN)_6] \cdot H_2O$ (2). Platelike yellow single crystals were obtained by slow evaporation of an aqueous solution (10 mL) of $GdCl_3 \cdot 6H_2O$, caprolactam, and $K_3[Cr(CN)_6]$ in a molar ratio of 1:2:1. Anal. Calcd for $C_{18}H_{32}CrGdN_8O_7$: C, 31.71; H, 4.73; N, 16.44. Found: C, 31.48; H, 4.60; N, 16.18. IR (KBr, cm^{-1}): 2150s, 2137s, 2127s ($\nu_{C/N}$); 1641, 1619 ($\nu_{C=O}$).

$[Gd(capro)_2(H_2O)_2Cr(CN)_6]$ (2′). **2′** was prepared by heating 100 mg of **2** at 120 °C for 2 h. Anal. Calcd for $C_{18}H_{26}CrGdN_8O_4$: C, 34.44; H, 4.17; N, 17.85. Found: C, 34.25; H, 4.32; N, 17.52. IR (KBr, cm^{-1}): 2147s, 2162w, 2128w ($\nu_{C/N}$); 1646, 1616 ($\nu_{C=O}$).

X-ray Structure Determination. The data collections of **1** and **2** were made at 293 K on Bruker Siemens *P*4 and Nonius Kappa-CCD diffractometers, respectively. The structures were solved by the direct method (SHELXS-97) and refined by full-matrix least-squares (SHELEXL-97) on F^2. Anisotropic thermal parameters were used for the non-hydrogen atoms and isotropic parameters for the hydrogen atoms. Hydrogen atoms were added geometrically and refined using a riding model. Weighted *R*-factors, wR, and all goodness of fit (*S*) values are based on F^2; conventional *R*-factors are based on *F*, with *F* set to zero for negative F^2. The weighting scheme is $w = 1/[\sigma^2(F_o^2) + (0.0433P)^2 + 0.0000P]$, where $P = (F_o^2 + 2F_c^2)/3$. One nitrogen atom of the coordinated urea ligands in **1** experiences serious disorder over two positions (N13 and N13′), and a split-atom model with a 1:1 occupancy was applied. The final Fourier map of **1** showed some residual peak and hole in the vicinity of the Gd atom (1.414/−2.106 e Å^{-3}), which is quite normal for complexes containing heavy metals. The crystal data are summarized in Table 1.

(17) Cruser, F. V. D.; Miller, E. H. *J. Am. Chem. Soc.* **1906**, *28*, 1132.

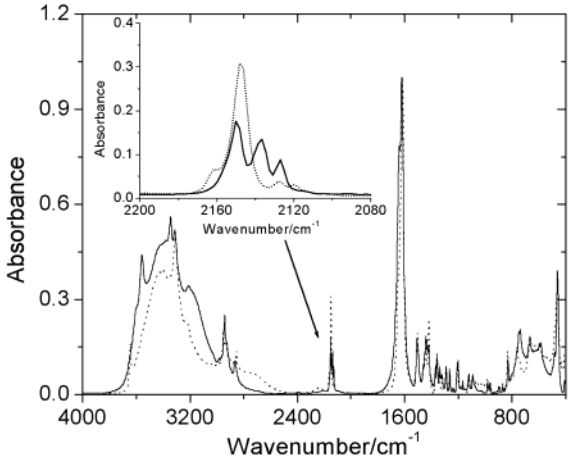

Figure 1. IR spectra of **2** (−) and **2′** (···). Inset: expansion of the spectra in the range 2200−2080 cm^{-1}.

Results and Discussion

Synthesis and Physical Characterizations. The two cyano-bridged GdCr complexes were synthesized by the assembly of Gd^{3+}, caprolactam or urea, and $Cr(CN)_6^{3-}$ in aqueous solution. The employment of urea and capro is due to the fact that they have a strong affinity for the Gd(III) ion similar to that of DMF and DMA. Aromatic amine ligands could also be used for the synthesis,[9] while aliphatic amines could not because they cause the precipitation of $Gd(OH)_3$.

It can be seen that complex **1** has a formula similar to that of the 1D DMF complex $[Gd(DMF)_4(H_2O)_2Cr(CN)_6] \cdot H_2O$. The difference in structures is unexpected because the two ligands are very alike. The use of fewer capro molecules (Gd/capro = 1:2) was initially expected to form a 2D complex, similar to the 2D $[Gd(DMF)_2(H_2O)_3Cr(CN)_6] \cdot H_2O$. However, a 1D complex (**2**) was obtained instead. It is worth mentioning that the reaction between $GdCl_3 \cdot 6H_2O$, caprolactam, and $K_3[Cr(CN)_6]$ in a molar ratio of 1:1:1 instead of 1:2:1 also affords complex **2**.

The TGA of complex **2** shows a weight loss of 8.2% in the temperature range 70−96.4 °C, corresponding to three water molecules, probably one interstitial water (O(1w)) and two weakly coordinated water molecules (O(3w) and O(5w)). This partially dehydrated material (**2′**) is stable below 168 °C, above which the additional loss of water molecules ensues. The mass loss of 5.4% in the temperature range 168−199 °C corresponding to two water molecules may result from the loss of the remaining two coordinated water molecules. A successive mass loss was observed upon further heating, suggesting decomposition of the sample.

The IR spectrum of **2′** is different from that of **2** in the range 2000−2200 cm^{-1} ($\nu_{C/N}$) as shown in Figure 1. For **2′**, a strong peak at 2147 cm^{-1}, together with two weak peaks, is observed, suggesting that more cyano ligands in $[Cr(CN)_6]^{3-}$ are involved in bridging. The loss of two coordinated water molecules requires the coordination of the cyano nitrogen atoms of adjacent chains to meet the usual coordination number of eight for Gd^{3+}. This would probably yield a 2D

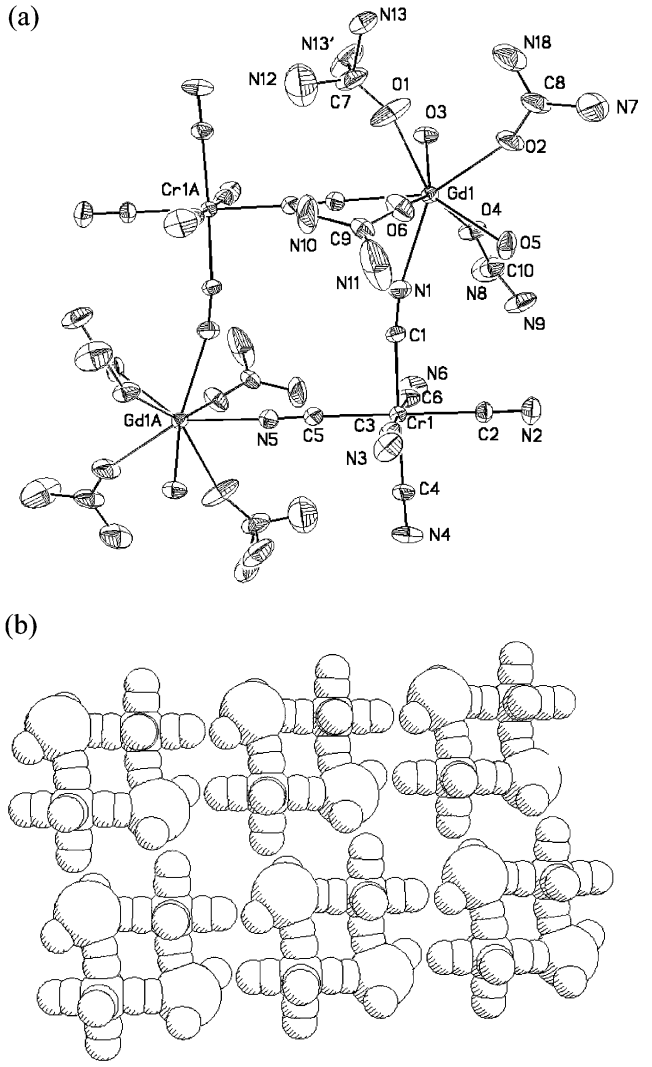

Figure 2. (a) Crystal structure of **1** showing the squarelike molecular structure. (b) Space filling diagram of **1** (urea ligands are omitted for clarification).

molecular structure.[18] The powder XRD pattern of **2′** is different from that of **2**, indicating that they possess different structures (see Supporting Information).

Interestingly, complex **2′** is quite soluble in water, and slow evaporation of the resultant solution gives rise to **2** as confirmed by elemental analyses.

$$\mathbf{2} \underset{+H_2O}{\overset{-H_2O}{\rightleftharpoons}} \mathbf{2'}$$

Crystal Structures. ORTEP drawings of complexes **1** and **2** are shown in Figures 2 and 3, respectively. Figure 4 shows the unit packing diagram of **2**. Selected bond distances and angles for **1** and **2** are listed in Tables 2 and 3, respectively.

The structure of **1** reveals that the complex is a neutral molecular square with two eight-coordinate Gd(III) ions linked by two $Cr(CN)_6$ moieties (Figure 2a). Each $Cr(CN)_6$ bridges two Gd(III) ions using two *cis* cyano ligands, and each Gd(III) ion in turn links two $Cr(CN)_6$ in a *cis* fashion

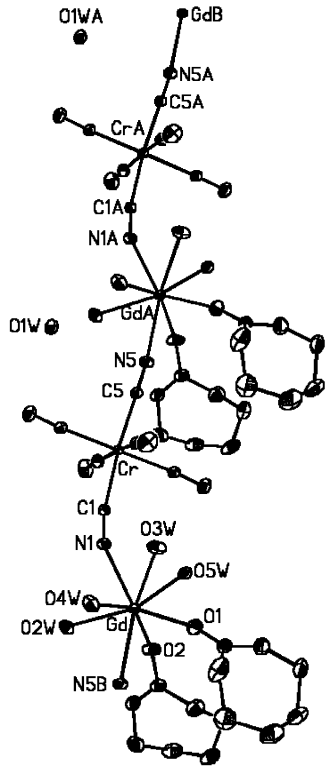

Figure 3. Chainlike structure of **2**.

as well, yielding a slightly distorted square. The bridging cyano ligands coordinate to the Gd(III) ion (Gd−N = 2.501(7) and 2.505(7) Å) in a bent fashion with the Gd−N≡C bond angles of 167.7(7)° and 170.2(8)°, respectively. The remaining coordination positions are occupied by six oxygen atoms of four urea and two water molecules with the Gd−O bond distances ranging from 2.319(6) to 2.454(6) Å. The largest distance between two atoms within the square is about 1.7 nm. The size of the molecular square is ca. 5.6×5.0 Å^2 (Figure 2b). The Cr−C bond distances and most of the Cr−C≡N bond angles are in the normal range, but the Cr−C≡N bonds that are involved in bridging exhibit distortion from linearity (172.3(7)° and 173.9(8)°). A similar situation occurs in complex **2** with N(1)−C(1)−Cr bond angle of 168.1(2)° (vide infra).

X-ray crystallography of **2** reveals that the structure consists of a 1D polymer $\{[Gd(capro)_2(H_2O)_4Cr(CN)_6]\cdot H_2O\}_n$, as shown in Figure 3. The chain is made of a cyano-bridged alternating $Cr(CN)_6$−$Gd(capro)_2(H_2O)_4$ fragment. The Gd atom is eight-coordinate with six oxygen atoms of four water molecules and two capro molecules and two nitrogen atoms of the bridging CN^- ligands bound to Gd(III). The bridging cyanides coordinate to the Gd(III) ion in a bent fashion with the bond angles of 152.9(2)° and 171.3(2)°. Each $Cr(CN)_6$ coordinates to two Gd(III) ions using two *trans* cyanide ligands, while each $Gd(capro)_2(H_2O)_4$ group connects two $Cr(CN)_6$ moieties in a *cis* fashion, yielding a zigzag chain structure.

In the crystal, the chains are connected through hydrogen bonds (Figure 4) between the unbridged cyano nitrogen atoms of one chain and the coordinated water molecules of the adjacent chains generating 1D cavities for the accom-

(18) Miyasaka, H.; Ieda, H.; Matsumoto, N.; Re, N.; Crescenzi, R.; Floriani, C. *Inorg. Chem.* **1998**, *37*, 255. Miyasaka, H.; Okawa, H.; Miyazaki, A.; Enoki, T. *J. Chem. Soc., Dalton Trans.* **1998**, 3991.

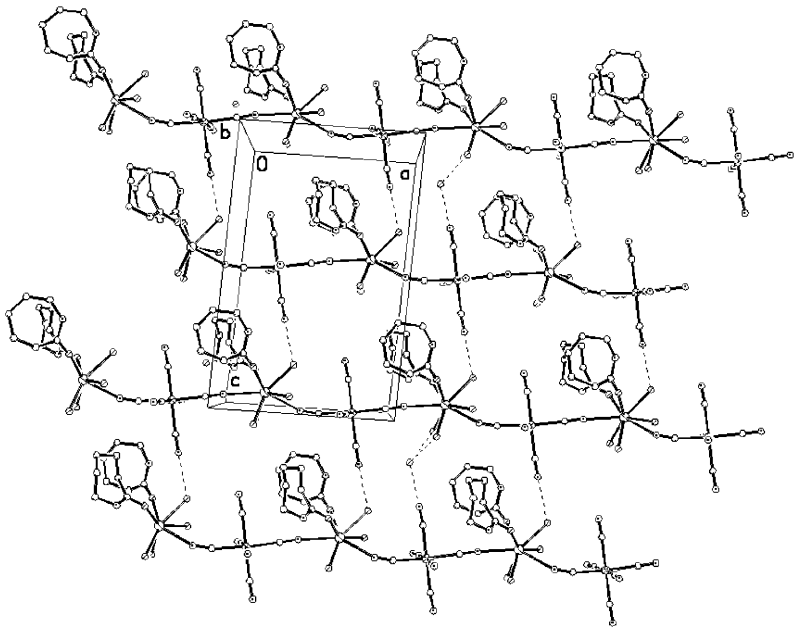

Figure 4. Hydrogen-bonded chains of **2** (along the *b* axis).

Table 2. Selected Bond Lengths (Å) and Angles (deg) for **1**[a]

Gd(1)−O(1)	2.378(7)	Gd(1)−O(2)	2.335(7)
Gd(1)−O(3)	2.440(5)	Gd(1)−O(4)	2.319(6)
Gd(1)−O(5)	2.454(6)	Gd(1)−O(6)	2.351(6)
Gd(1)−N(1)	2.505(7)	Gd(1)−N(5)#1	2.501(7)
Cr(1)−C(1)	2.066(8)	Cr(1)−C(2)	2.061(8)
Cr(1)−C(3)	2.066(9)	Cr(1)−C(4)	2.068(9)
Cr(1)−C(5)	2.075(8)	Cr(1)−C(6)	2.054(9)
C(5)−N(5)−Gd(1)#1	170.2(8)	C(1)−N(1)−Gd(1)	167.7(7)
N(5)#1−Gd(1)−N(1)	72.1(2)		

[a] Symmetry transformations used to generate equivalent atoms: #1 $-x+1, -y+1, -z+1$.

Table 3. Selected Bond Lengths (Å) and Angles (deg) for **2**[a]

Gd−O(1)	2.286(2)	Gd−O(2)	2.277(2)
Gd−O(3W)	2.477(2)	Gd−O(4W)	2.384(2)
Gd−O(5W)	2.431(2)	Gd−O(2W)	2.399(2)
Gd−N(1)	2.505(2)	Gd−N(5)#1	2.547(2)
Cr−C(1)	2.079(2)	Cr−C(2)	2.074(2)
Cr−C(3)	2.077(3)	Cr−C(4)	2.066(2)
Cr−C(5)	2.072(2)	Cr−C(6)	2.068(2)
C(5)−N(5)−Gd#2	171.3(2)	C(1)−N(1)−Gd	153.51(19)
N(5)#1−Gd−N(1)	145.75(7)		

[a] Symmetry transformations used to generate equivalent atoms: #1 $x+1, y, z$; #2 $x-1, y, z$.

modation of coordinated caprolactam molecules (see Supporting Information).

Magnetic Properties. Squarelike 1. The temperature dependence of the magnetic susceptibility for complex **1** shown in Figure 5 suggests the presence of antiferromagnetic coupling between the adjacent Gd(III)−Cr(III) ions. The Weiss constant derived from the χ_m^{-1} versus T plot is equal to −3.1 K with the Curie constant of 19.6 emu K mol^{-1}, in good agreement with the calculated value of 19.5 emu K mol^{-1} ($g = 2.0$) per Gd_2Cr_2. According to the crystal structure data, complex **1** is a tetranuclear entity, which requires four coupling constants. For simplicity, the coupling constants between the cyano-bridged Gd−Cr ions are assumed to be equal, and the diagonal coupling constants are

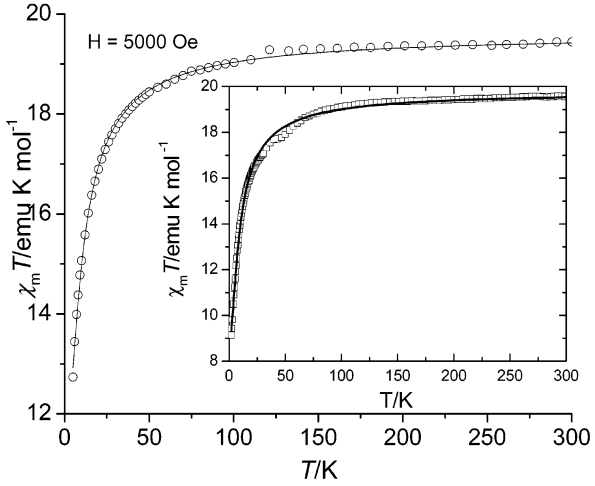

Figure 5. Temperature dependence of $\chi_m T$ for **1**. Inset: temperature dependence of $\chi_m T$ per Gd_2Cr_2 for **2**. The solid line is the best fit with the parameters in the text.

neglected because they are considerably small compared to that of a system with coupling through cyano bridges. On this basis, the appropriate Hamiltonian is

$$H = -2J(S_{Gd(1)}S_{Cr(3)} + S_{Gd(1)}S_{Cr(4)} + S_{Gd(2)}S_{Cr(3)} + S_{Gd(2)}S_{Cr(4)}) \quad (1)$$

where J is the coupling through the cyano bridges. The corresponding expression derived by the Kambe's method,[19] together with a molecular field term that describes the intercluster magnetic interaction (j'), is used to fit the experimental data giving the following results: $J = -0.36$ cm^{-1}, $g = 2.00$, $zj' = +0.031$ cm^{-1} (z is the number of the next-nearest clusters around a designated cluster, 4 in the present case), and $R = \sum(\chi_{obsd}T - \chi_{calcd}T)^2/\sum(\chi_{obsd}T)^2 = 1.7 \times 10^{-5}$.

(19) Kambe, K. *J. Phys. Chem. Jpn.* **1950**, *5*, 48.

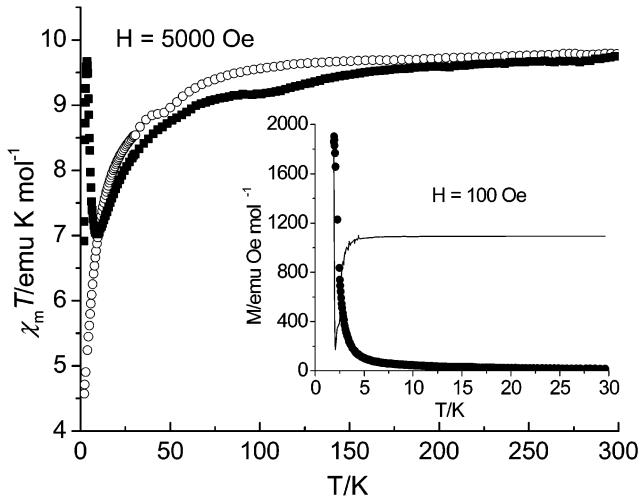

Figure 6. Temperature dependence of $\chi_m T$ for **2** (○) and **2′** (●) per GdCr. Inset: plot of field-cooled magnetization (FCM) vs temperature measured in 100 Oe for **2′**. The solid line represents the d(FCM)/dT derivative.

Previous experimental data have shown that most of the transition metal−Gd(III) complexes exhibit ferromagnetic coupling, which is explained by the 3d to 5d charge transfer.[20,21] A weak antiferromagnetic interaction observed in the oxalate-bridged Cr(III)−Gd(III) complex was assigned to the long Cr···Gd distance and/or the larger energy costs for charge-transfer transitions from the 3d orbital of Cr(III) to the 5d orbital of Gd(III) than those of M(II) ions.[22] The comparatively stronger intermetallic antiferromagnetic interaction relative to that of the oxalate-bridged dinuclear Cr−Gd complex may be due to the comparatively smaller intermetallic separations in **1** and/or stronger magnetic coupling propagated by the cyano ligands.

Another feature is that spin frustration may exist in the tetranuclear cluster if the magnitude of the diagonal coupling is comparable to the J value. However, the FCM and ZFCM measurements showing no divergence down to 1.8 K dismiss such a possibility. This shows that the diagonal coupling is weaker than the magnetic exchange through cyano bridges, and the negligence of the former factor during the theoretical treatment is reasonable.

Chainlike 2 and Soluble Magnet 2′. The plots of $\chi_m T$ versus T (per GdCr unit) for **2** and **2′** also confirm the antiferromagnetic interactions between adjacent Gd(III)···Cr(III) ions (Figure 6). The anomaly at 50 K is owing to the presence of molecular oxygen in the samples. The magnetic susceptibilities above 10.0 K obey the Curie−Weiss law with negative Weiss constants, θ, of −4.5 K for **2** and −6.3 K for **2′**, suggestive of the existence of antiferromagnetic coupling between the adjacent Gd(III) and Cr(III) ions. The Curie constant, C, is equal to 10.0 emu K mol^{-1} for both complexes, close to the expected value of 9.75 emu K mol^{-1} with $g = 2.0$. The temperature dependence of zero-DC field AC magnetic susceptibilities for complex **2** shows that the in-phase component (χ') has no maximum down to 1.8 K, and the out-of-phase component (χ'') stays at zero, indicating that no magnetic ordering occurs down to 1.8 K. The presence of a minimum in $\chi_m T$ indicates the ferrimagnetic nature of **2′** as a result of the existence of the noncancellation of spins and larger Gd(III)−Cr(III) magnetic coupling compared to **2**.

Because there is no theoretical expression used to fit the magnetic data of 1D systems with alternating $S = {}^7/_2$ and ${}^3/_2$, Ribas et al. have recently employed a Gd_3Cr_3 hexagon to simulate the magnetic susceptibilities of infinite GdCr chains on the condition that J is small. According to them, a Gd_2Cr_2 square should approximately describe the behavior of chainlike complex **2** as well. The fit to the experimental data gives the following results: $J = -0.33$ cm^{-1}, $g = 2.02$, $zj' = -0.015$ cm^{-1}, and $R = \sum(\chi_{obsd} - \chi_{calcd})^2/\sum(\chi_{obsd})^2 = 8.3 \times 10^{-4}$ (inset of Figure 5). The absolute J value is comparable to that of complex **1** and other cyano-bridged 1D Gd(III)−Cr(III) complexes.[10b]

The FCM curve of **2′** in 100 Oe (inset of Figure 6) displays an abrupt increase at 2 K. The derivative curve, d(FCM)/dT, presents an extremum at 2.1 K, corresponding to the transition temperature (T_c). Similar to the FCM curve, the ZFCM curve exhibits a similar transition at ca. 2.1 K (See Supporting Information). The existence of a magnetic transition is also confirmed by the isothermal magnetization measurements discussed later. The hysteresis loop at 1.8 K shows the presence of small coercive field of ca. 10 Oe, which is typical of a molecular magnet. The small coercive field is not unexpected considering that both metal ions in the complex are isotropic. The occurrence of spontaneous magnetization evidences a multidimensional network in **2′**. Unfortunately, no single crystals suitable for X-ray structural analysis were obtained because the loss of water results in the collapse of the crystal lattice. Powder XRD measurements together with the infrared spectra clearly show the great difference in structures of **2** and **2′**, which is strongly supported by the magnetic results. It is worth noting that the desolvation of discrete cyano-bridged [Mn(SB)(solvent)]$_2$[Fe(CN)$_6$]$^-$ trinuclear and ionic [Mn(SB)(solvent)$_2$]$^+$−[Fe(CN)$_6$]$^{3-}$ (SB = Schiff base) complexes results in cyano-bridged 2D species exhibiting long-range magnetic ordering.[18]

Isothermal Magnetization. The field dependence of the magnetization (0−70 kOe) of **2′** measured at 1.8 K shows saturation of the magnetization (Figure 7), reaching the expected value of 4.0 Nβ at 2.3 T for antiferromagnetic Gd(III)−Cr(III) systems with $S_T = {}^7/_2 - {}^3/_2 = 2$. This also confirms the $S = 2$ ground state for the complex. For ferro- or ferrimagnets, the magnetization increases rapidly to reach saturation at low field. The rapid increase in the magnetization at low field for **2′** is typical of the presence of 3D magnetic ordering similar to that of the 2D metamagnet [Gd(DMF)$_2$(H$_2$O)$_3$Cr(CN)$_6$]·H$_2$O,[10] while the regular increase for

(20) Carlin, R. L.; Vaziri, M.; Benelli, C.; Gatteschi, D. *Solid State Commun*. **1988**, *66*, 79. Bencini, A.; Benelli, C.; Caneschi, A.; Carlin, R. L.; Dei, A.; Gatteschi, D. *J. Am. Chem. Soc.* **1985**, *107*, 8128. Bencini, A.; Benelli, C.; Caneschi, A.; Dei, A.; Gatteschi, D. *Inorg. Chem.* **1986**, *25*, 572.
(21) Sakamoto, M.; Manseki, K.; Okawa, H. *Coord. Chem. Rev.* **2001**, *219−221*, 379 and references therein.
(22) Sanada, T.; Suzuki, T.; Yoshida, T.; Kaizaki, S. *Inorg. Chem.* **1996**, *37*, 4712.

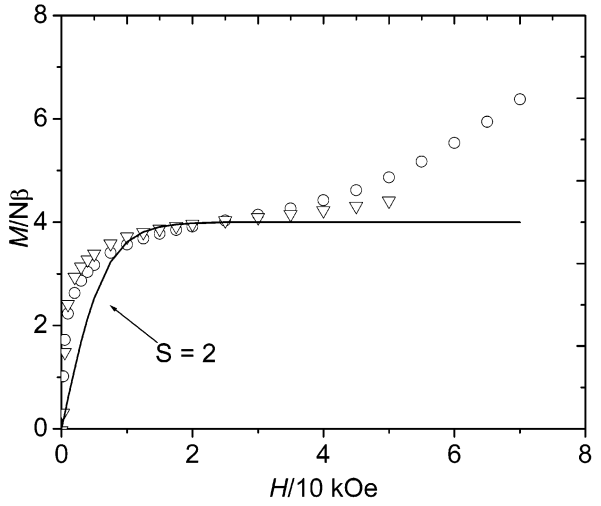

Figure 7. Field dependence of magnetization at 1.8 K for **2′** (○) and [Gd(DMF)$_2$(H$_2$O)$_3$Cr(CN)$_6$]·H$_2$O[10] (▽). The solid line represents the Brillouin function that corresponds to $S = 2$ state with $g = 2.0$.

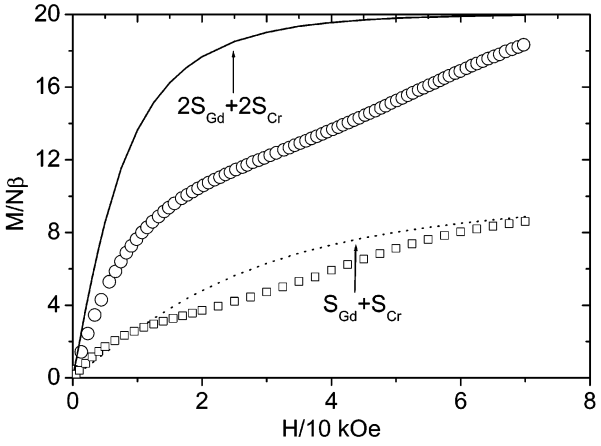

Figure 8. Field dependence of magnetization at 1.84 K for **1** (○) and at 1.8 K for **2** (□). The lines represent the Brillouin function that corresponds to noninteracting $S = S_{Gd} + S_{Cr}$ (− for **2**) and $S = 2S_{Gd} + 2S_{Cr}$ ions (··· for **1**) with $g = 2.0$.

2 (Figure 8) indicates the paramagnetic properties with a degree of antiferromagnetic intermetallic coupling.

Compared to the theoretical Brillouin curve for an $S = 2$ spin state with $g = 2.0$, the experimental data of **2** are in good agreement with the Brillouin curve at low fields (below 20 kOe); however, those of **2′** exhibit deviation suggesting the presence of ferrimagnetic ordering. Similar to **2**, the experimental curve for complex **1** lies below the Brillouin curve corresponding to noninteracting S_{Gd} and S_{Cr} spins (Figure 8), suggesting the paramagnetic state of the two complexes with weak intermetallic antiferromagnetic exchange.

With the further increase of the applied field, the magnetization increases again, attaining 6.2 Nβ for **2′** at 70 kOe (Figure 7). This behavior implies that the initial antiparallel spins (S_{Gd} and S_{Cr}) turn parallel although the magnetization has not reached the expected saturation value of 10 Nβ for ideal parallel alignment of the local spins, which might require higher external field. Significantly, similar phenomena have been observed in other cyano-bridged Gd(III)−Cr(III) complexes, for example, 2D [Gd(DMF)$_2$(H$_2$O)$_3$Cr(CN)$_6$]·H$_2$O[10] (4.4 Nβ at 50 kOe) and 3D GdCr(CN)$_6$·4H$_2$O (ca. 4.8 Nβ (1.3 K) at 130 kOe).[8] These results are in good agreement with the increasing order of the magnitude of Gd−Cr antiferromagnetic interaction (Weiss constants: −6.3 K for **2′**, −8.5 K for [Gd(DMF)$_2$(H$_2$O)$_3$Cr(CN)$_6$]·H$_2$O, −12 K for GdCr(CN)$_6$·4H$_2$O). The weaker the antiferromagnetic coupling the easier is the reversal of local spins. This reveals that the Gd(III)−Cr(III) antiferromagnetic coupling is comparatively weak and could be overcome by an external magnetic field with the magnitude strong enough. Significantly, this behavior has not been observed in other 3D cyano-bridged 4f−3d ferrimagnets,[8] most of which have weak magnetic exchange between 4f and 3d ions because of the effective shielding of 4f electrons by the outer-shell electrons.

In conclusion, a new cyano-bridged chainlike and a novel squarelike Gd(III)−Cr(III) complex have been synthesized and characterized by single-crystal X-ray and magnetic investigations. The magnetic square is one of the few neutral ones known to date,[23] and it is the only example containing the hexacyanometalate moiety that tends to form extended or linear polynuclear arrays. The present nanoscaled molecular square further emphasizes the structural diversity of hexacyanometalate. The Cr(III)−Gd(III) magnetic coupling has been accurately evaluated to be −0.36 cm^{-1} in magnitude for the first time. Significantly, a soluble ferrimagnet has been characterized. Field dependences of magnetization for the GdCr complexes show unusual field-induced metamagnetic behavior from the *ferrimagnetic* ground state to *ferromagnetic* state.

Acknowledgment. This work was supported by the National Natural Science Foundation of China (20151001). H.Z.K. also thanks Tsinghua University for supporting this work.

Supporting Information Available: Hydrogen-bonded chains showing the cavities of **2** (along the *a* and *c* axes). Powder XRD patterns of complex **2′** and **2** (calculated). TGA curve of **1**. An X-ray crystallographic file (CIF). Hysteresis loop at 1.8 K and ZFCM for **2′**. This material is available free of charge via the Internet at http://pubs.acs.org.

IC025704J

(23) Oshio, H.; Tamada, O.; Onodera, H.; Ito, T.; Ikoma, T.; Tero-Kubota, S. *Inorg. Chem.* **1999**, *38*, 5686. Galan-Mascaros, J. R.; Dunbar, K. R. *Chem. Commun.* **2001**, 217. Harada, K.; Yuzurihara, J.; Ishii, Y.; Sato, N.; Kambayashi, H.; Fukuda, Y. *Chem. Lett.* **1995**, 887.